

Characteristics of lead glass for radiation protection purposes: A Monte Carlo study

M. Zadehraf^{1,2*}, C. Olaru¹, S.A. Ciobanu¹, G.V. Ormenisan¹

¹Horia Hulubei National Institute for Research and Development in Physics and Nuclear Engineering, Bucharest-Magurele, Romania

²Department of Physics, Faculty of Basic Science, University of Mazandaran, Babolsar, Iran

ABSTRACT

Background: Lead glass has a wide variety of applications in radiation protection. This study aims to investigate some characteristics of lead glass such as the γ -ray energy-dependent mass and linear attenuation coefficients, the half-value layer thickness, and the absorbed dose distribution for specific energy. **Materials and Methods:** The attenuation parameters of different lead glass types against high-energy photons (0.2-3 MeV) of gamma rays have been calculated by the Monte Carlo technique and a deterministic method. Besides, the depth dose distribution inside the volume of two cubic lead glass samples was calculated by two Monte Carlo-based computer codes, for gamma rays of 300 keV. In each part of the study, the results of the two methods have been compared. **Results:** Increasing the Pb concentration (weight in %) by 1% in the lead glass causes a 1.6%-3% increase in the linear attenuation coefficient, depending on the energy. However, the mass attenuation coefficient does not show significant variation for different types of lead glass, especially for the energies higher than 400 keV. Moreover, almost half of the total dose from 300 keV photons will be absorbed in the first 3.5 mm of the sample's thickness. **Conclusion:** Results indicate that the Monte Carlo technique is as reliable as the deterministic methods for calculating the attenuation characteristics of the lead glass. The provided data in this investigation can be useful for radiation protection purposes, especially in the case of selecting the lead glass type and dimension based on a specific application.

Keywords: γ -ray attenuation, radiation shielding, dose distribution, lead glass, Monte Carlo.

► Short report

*Corresponding authors:

Dr. Mastaneh Zadehraf,

E-mail:

mastaneh.zadehraf@nipne.ro

Revised: July 2020

Accepted: July 2020

Int. J. Radiat. Res., October 2020;
18(4): 907-912

DOI: 10.18869/acadpub.ijrr.18.4.895

INTRODUCTION

While working with the ionizing radiation, the protection of living organisms and sensitive equipment against the hazard of radiation is crucially needed. This protection can be done in terms of dosimetry and/or shielding against ionizing radiation. Shielding an experimental setup containing radioactive sources, with a suitable transparent shielding material will protect the experimenter personnel from the hazard as well as preventing the experiment results from the environmental interference, without losing the visual contact.

Photon-matter interaction parameters such as linear and mass attenuation coefficients and half-value layer thickness (HVL) can provide some information to evaluate the performance of the radiation shielding materials. One of the most commonly used materials in radiation shielding applications is lead glass. Being both transparent and good attenuator of high energy photons (due to their high density and atomic number), different types of lead glass can be applied as viewing windows at radioactive storage stations, hot cells, nuclear fuel development and reprocessing plants, and for the applications related to nuclear reactors ^(1, 2).

Furthermore, all the widely spread radiotherapy centers are using lead glass as the observation window, while ensuring the protection of personnel from being overexposed to the ionizing radiation (3). Therefore, studying the photon attenuation characteristics of the lead glass as a radiation-shielding material is an important subject in medical physics and other radiation-related nuclear fields (1-3).

Besides being a very good radiation-shielding material, lead glass can also provide important radiation protection –related dosimetric data, which means it can be used as a passive reusable solid-state dosimeter (4,5). When a glass sample (lead glass in this case) is exposed to the ionizing radiation, some of its parameters (like color) will change (6). In other words, exposure to a particular dose of ionizing radiation causes a proportional darkening in the lead glass and affects its transparency (7). These changed parameters are proportional to the absorbed dose by the sample (8, 9). Investigation on radiation-shielding properties of different types of glass has been performed before for some photon energies (10-12). However, studies regarding a wide energy region with the most commonly used lead glasses, which cover both dosimetry and radiation-shielding applications are very scarce. There have been also studies on the dose-related variation of the optical properties of glass samples (13). As is known, the absorbed dose is correlated with the radioactive source type and energy, the density and elemental composition of the absorber, and the source-absorber distance. Therefore, it is important to choose the optimum density and thickness of the lead glass, to maintain both transparency and shielding characteristics.

This work aims to investigate the attenuation properties of different types of the lead glass (ZF1, ZF2, ZF3, ZF6, and ZF7) against γ -rays of 0.2-3 MeV energies, as well as the dose distribution through the volume of cubic samples of ZF1 and ZF7, for gamma rays of 300 keV energy. The attenuation characteristics provide useful information on the shielding applications of the lead glass, and the dose distribution results can be useful in dosimetry applications.

MATERIALS AND METHODS

Attenuation parameters

The characteristics of the five types of lead glass are presented in table 1. The mass fractions (weight in %) of the main components (SiO_2 and PbO) as well as the other materials (K_2O , As_2O_3 , etc.) are provided in this table. Since lead is a heavy and opaque element, it is obvious that increasing the Pb concentration leads to more density and less transparency in the glass samples.

Table 1. Characteristics of the five types of lead glass.

lead glass type	density (g/cm^3)	SiO_2 (Weight in %)	PbO (Weight in %)	other materials (Weight in %)	transparency (%)
ZF1	3.86	41.20	51.20	7.60	95
ZF2	4.12	39.10	55.41	5.49	90
ZF3	4.46	33.88	61.05	5.07	85
ZF6	4.77	30.96	65.06	3.98	75
ZF7	5.19	27.27	70.93	1.8	70

To calculate the attenuation parameters, a Monte Carlo-based computer code (MCNP-4C) has been applied. MCNP is a general-purpose Monte Carlo N-Particle transport code, which is developed and maintained by Los Alamos National Laboratory (14,15). The geometry setup, consisting of two cylindrical collimators made of pure lead (source and detector collimators) and a detection area, is identical to figure 1 of the ref. (16). A disk-shaped sample of 1 cm thickness and 8 cm diameter, made of lead glass is located between the source and detector collimators. Point-like monoenergetic gamma sources in the energy range of 0.2-3 MeV with 200 keV increments have been located at the entrance of the source collimator, to obtain the attenuation parameters as a function of energy.

To obtain the flux over the detector cell, the F4 tally of MCNP-4C has been used. F4 is a special tally for track length estimation of cell flux. The number of tracked photons (events) was considered as 10^7 in each simulation process. For each energy value, the theoretical experiments were performed six times, for five types of the lead glass (ZF1, ZF2, ZF3, ZF6, and ZF7). At first, the simulation was done with no sample between the collimators, and the result

of F4 tally was registered as the photon flux over the detector cell, in the absence of the attenuator (known as incident photons). Then, the simulation was repeated in the presence of each sample type individually, to obtain the flux of the transmitted photons. Therefore, the linear attenuation coefficient (μ) can be determined by equation (1) ⁽¹⁷⁾.

$$\mu = \frac{1}{x} \ln\left(\frac{N_0}{N}\right) \quad (1)$$

Where; N_0 , N , and x are the incident photons, transmitted photons, and the sample thickness, respectively.

The mass attenuation coefficient (μ_p), an independent parameter of the material density, is defined by equation (2) ⁽¹⁷⁾.

$$\mu_p = \frac{\mu}{\rho} \quad (2)$$

In equation (2), ρ is the material density in the unit of (g/cm^3) and μ is the linear attenuation coefficient in the unit of (cm^{-1}), obtained from equation (1). For the mass attenuation coefficient, the simulation results have been compared with the results of the XCOM ⁽¹⁸⁾ program. This comparison can be a validation of the modeling process. Furthermore, one can obtain a continuous mass attenuation graph by using XCOM, which may be applicable for any energy value by extrapolation of the graph. The XCOM program is freely available on the National Institute of Standards and Technology (NIST) website ⁽¹⁹⁾.

The half-value layer thickness (HVL) (equation 3), is defined as the thickness of the attenuator that reduces the intensity of photons by half of its initial magnitude ⁽¹²⁾:

$$HVL = \frac{\ln(2)}{\mu} \quad (3)$$

Dose distribution as a function of depth inside a sample

In the second part of the study, a cubic sample of $1 \times 1 \times 1 \text{ cm}^3$ has been considered to investigate the dose distribution as a function of depth inside the volume of the lead glass. The dimension of the sample is chosen arbitrarily. A

point-like monoenergetic gamma source of 300 keV energy was located at 100 cm distance from the center of the mass of the sample. MCNP-4C and EGSnrc codes have been applied to perform the simulation. EGSnrc was originally released in 2000, as a complete overhaul of the Electron Gamma Shower (EGS) software package originally developed at the Stanford Linear Accelerator Center (SLAC) in the 1970s ⁽²⁰⁾. The calculation has been performed for ZF1 and ZF7 (as two extrema of the Pb concentration among the five models mentioned in table 1). The cubic lead glass sample was divided into ten identical layers of 1 mm thickness. Using the simulation codes, the total dose absorbed by each layer of the main cube has been calculated. Having a quite small sample of lead glass (each layer is $1 \times 1 \times 0.1 \text{ cm}^3$), the number of tracked particles was set at 10^8 in this part of the work, to reduce the relative error to a reasonable value (less than 0.1). Since Monte Carlo is a statistical-based technique, extensive statistical analysis for outputs is applied in each code. For example, ten statistical checks in MCNP are made with a pass yes/no criterion to assess the tally convergence, relative errors, figure of merit, etc. The relative error is inversely related to the number of histories and must be less than 0.1 to be evaluated as a reliable output.

RESULTS

The linear attenuation coefficients for ZF1, ZF2, ZF3, ZF6, and ZF7 glasses are plotted in figure 1(a) as a function of gamma-ray energy, for the energy interval 0.2-3 MeV with 200 keV increments. According to data presented in table 1 and figure 1(a), the average increasing rate of linear attenuation coefficient (in percent) has been obtained related to a 1% increase of the PbO concentration (in terms of the mass fraction) in the lead glass sample and is shown in figure 1(b).

The mass attenuation coefficients as a function of gamma-ray energy are plotted in figure 2(a), for the same energies as figure 1. Since the mass attenuation coefficient is

independent of the material density, one can observe just a slight difference in mass attenuation coefficients between various types of lead glass, due to different elemental concentrations.

A comparison between the mass attenuation coefficients calculated by the Monte Carlo method (MCNP-4C) and the ones obtained from XCOM shows a very good agreement between the two different methods (figure 2(b)).

The half-value layer thicknesses (HVL) have been calculated for ZF1, ZF2, ZF3, ZF6, and ZF7, using the equation (3) and the results are illustrated in figure 3.

To investigate the depth dose distribution inside the volume of each sample, the

percentage of the total dose absorbed by each layer inside the main cube, for ZF1 and ZF7 and photons of 300 keV energy has been calculated. The results of simulation by MCNP-4C and EGSnrc are shown in figure 4. It can be found from this figure that in the first 3.5 mm thickness of the main cube, more than 45% and 55% of the total dose will be absorbed in ZF1 and ZF7 cubic samples of $1 \times 1 \times 1$ cm³, respectively. This figure also shows the accordance of the results obtained by two different simulation codes, both working based on the Monte Carlo technique. The observed discrepancy between the results of MCNP-4C and EGSnrc for photons of 300 keV energy was no more than 3% for both ZF1 and ZF7.

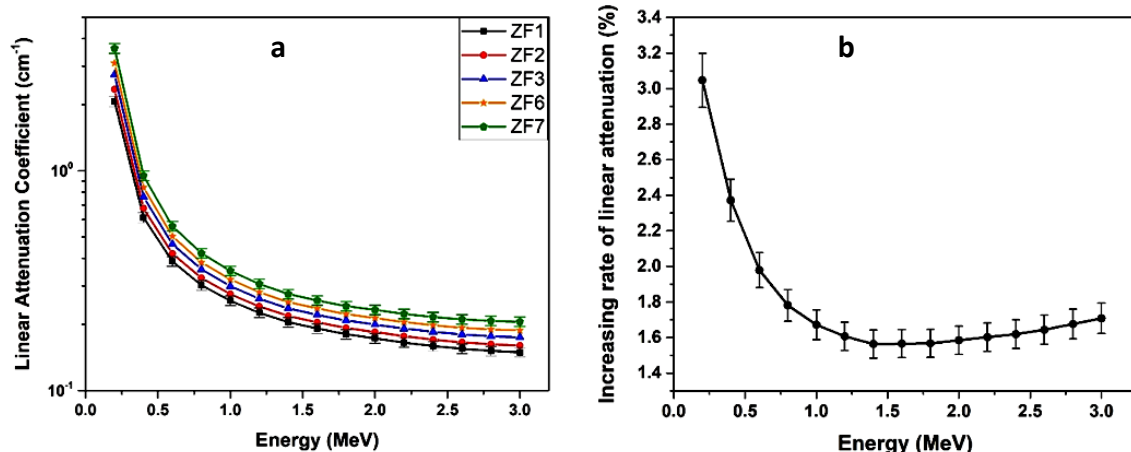


Figure 1. (a) Linear attenuation coefficients for five types of lead glass as a function of energy. (b) The average increasing rate of the linear attenuation coefficient (in percent) for a 1% increase of the PbO concentration in lead glass, as a function of energy.

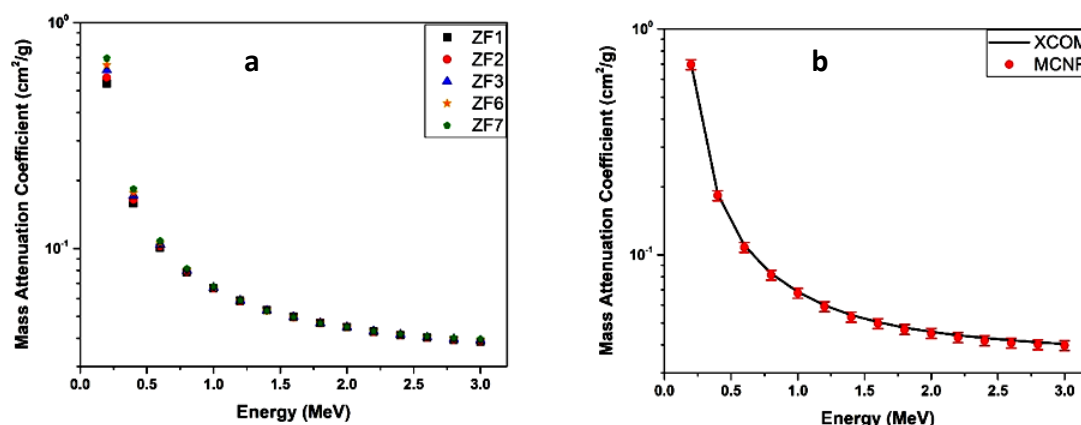


Figure 2. (a) Mass attenuation coefficients for five types of lead glass as a function of energy. (b) Comparison between mass attenuation coefficients obtained by MCNP-4C and XCOM, for ZF7.

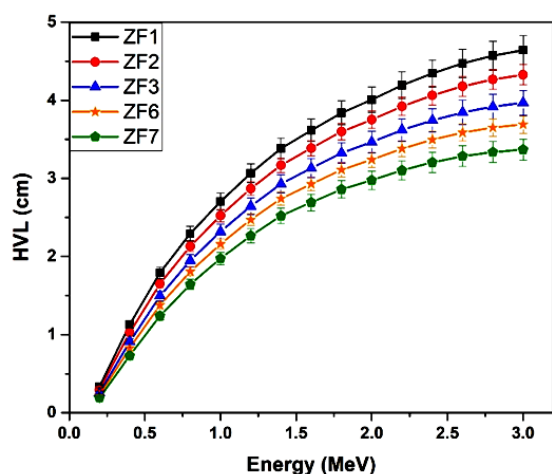


Figure 3. Half-value layer thicknesses for five types of lead glass as a function of energy.

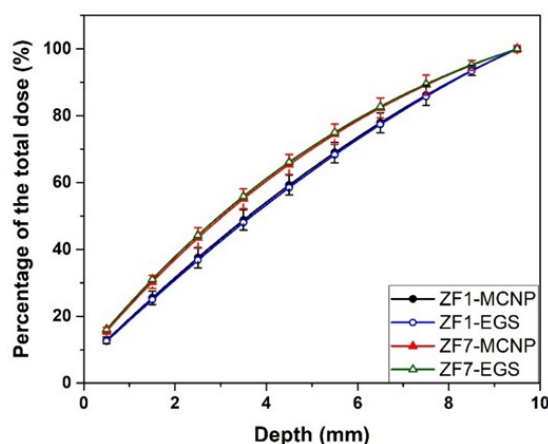


Figure 4. The percentage of the total dose, absorbed by each layer inside the cubic samples of ZF1 and ZF7 (% dose) for gamma rays of 300 keV energy. The simulation was done by MCNP-4C and EGSnrc.

DISCUSSION

As can be seen in figures 1(a) and, the linear and mass attenuation coefficients show an exponential decrease by increasing the energy of gamma rays, which is in agreement with refs. (3, 10, 12). Furthermore, increasing the concentration of Pb as a heavy element leads to a higher attenuation coefficient in these glasses. Figure 1 (b) reveals this increasing rate.

It can be found from figure 1(b) that for the photons of 200 keV energy, increasing the lead concentration by 1% causes an averagely increase in the linear attenuation by around 3%. While the gamma-ray energy increases, this

increasing rate drops drastically. In the energy range of 0.8-3 MeV, the increasing rate of linear attenuation is less than 2%, for an increased Pb concentration by 1%. Indeed, the maximum (3%) and minimum (1.6%) increasing rates in this energy interval happen for 200 keV and 1.4 MeV, respectively.

For the energy values of 0.2, 0.4, 0.6, and 0.8 MeV, the mass attenuation coefficient of ZF7 (with the highest Pb concentration) compared to ZF1 (with the lowest Pb concentration) has increased by 29.6%, 15.4%, 7.6%, and 3.8%, respectively. However, in the energy range of 1-3 MeV, the relative difference between the mass attenuation coefficients of ZF1 and ZF7 is less than 2.5% (figure 2(a)).

Figure 2(b) is presented for a comparison between MCNP and XCOM as a deterministic method. The results of the two methods for all types of lead glass and in the interested energy interval comply with each other very well (less than 4% discrepancy). For brevity, this comparison is just shown for ZF7 in figure 2(b). The attenuation coefficients are higher in the low energy range in which the photoelectric effect is dominant. Then they show a rapid decrease by increasing the energy to the range corresponding to the Compton scattering region (figures 1(a) and 2).

CONCLUSION

Using the results of this study and based on both transparency and attenuation properties needed for a specific application of the lead glass, one can select the optimum concentration of the lead for a desired model. This study also shows that the Monte Carlo technique is as reliable as the deterministic methods for calculating the shielding parameters of lead glass at the interested energy interval. The provided results and data in this work can be used as references or comparable values for radiation protection purposes, in terms of both dosimetry and shielding applications.

Conflicts of interest: Declared none.

REFERENCES

1. Manohara SR, Hanagodimath SM, Gerward L (2009) Photon interaction and energy absorption in glass: a transparent gamma ray shield. *J Nucl Mater*, **393(3)**: 465–472.
2. Kim ST, Kim J, Park JM (2019) Radiation dose assessment for radiation workers during 18F-FDG synthesis and dispensing activities in hot cells: a proposal to improve the safety of radiation protection measures for workers. *Int J Radiat Res*, **17(4)**: 587-593.
3. Fathi FM (2006) Mass attenuation of gamma photons in special lead glass that can be used in radiation shielding windows. *Raf Jour Sci*, **17(2)**: 6-12.
4. Ioan MR (2016) Study of the optical materials degradation caused by gamma radiation and the recovery process by controlled heat treatment. *Rom J Phys*, **61(5-6)**: 892-902.
5. Ioan MR (2016) Analyzing of the radiation induced damage to optical glasses by using online heating laser measurements. *Rom J Phys*, **61(3-4)**: 614-625.
6. Ioan MR, Gruia I, Ioan G-V, Rusen L, Ioan P (2014) Laser beam used to measure and highlight the transparency changes in gamma irradiated borosilicate glass. *J Optoelectron Adv M*, **16(1-2)**: 162-169.
7. Ioan MR, Gruia I, Ioan P, Bacalaum M, Ioan G-V, Gavrila C (2013) 3 MeV protons to simulate the effects caused by neutrons in optical materials with low metal impurities. *J Optoelectron Adv M*, **15(5-6)**: 523-529.
8. Ioan MR (2016) LIDT test coupled with gamma radiation degraded optics. *Opt Commun*, **369**: 94-99.
9. Ioan MR (2016) Investigation of RGB spectral components in the images captured through gamma rays affected optical focusing lens. *Rom J Phys*, **61(7-8)**: 1198-1206.
10. Kurudirek M, Özdemir Y, Şimşek Ö, Durak R (2010) Comparison of some lead and non-lead based glass systems, standard shielding concretes and commercial window glasses in terms of shielding parameters in the energy region of 1 keV-100GeV: A comparative study. *J Nucl Mater*, **407(2)**: 110-115.
11. Limkitjaroenporn P, Kaewkhao J, Limsuwan P, Chewpraditkul W (2011) Physical, optical, structural and gamma-ray shielding properties of lead sodium borate glasses. *J Phys Chem Solids*, **72(4)**: 245-251.
12. Singh N, Singh KJ, Singh K, Singh H (2006) Gamma-ray attenuation studies of PbO-BaO-B₂O₃ glass system. *Radiat Meas*, **41(1)**: 84-88.
13. Arbuzov VI, Andreeva NZ, Leko NA, Nikitina SI, Orlov NF, Fedorov YK (2005) Optical, spectral, and radiation-shielding properties of high-lead phosphate glasses. *Glass Phys Chem*, **31(5)**: 583–590.
14. <https://mcnp.lanl.gov> (accessed July 3, 2020).
15. Briesmeister JF (Ed.) (2000) MCNPTM – A General Monte Carlo N-Particle Transport Code, LA-13709-M, V4C.
16. El-Khayatt AM, Ali AM, Singh VP, Badiger NM (2014) Determination of mass attenuation coefficient of low-z dosimetric materials. *Radiat Eff Defect S* **169**: 1038-44.
17. Hubbell JH (1982) Photon mass attenuation and energy-absorption coefficients from 1 keV to 20 MeV. *Int J Appl Radiat Isot* **33**: 1269–1290.
18. Berger MJ, Hubbell JH, Seltzer SM, Chang J, Coursey JS, Sukumar R, Zucker DS, Olsen K (last update: 2010) NIST Standard Reference Database 8 (XGAM). *NIST, PML, Radiation Physics Division*. Originally published as NBSIR 87-3597.
19. <https://physics.nist.gov/PhysRefData/Xcom/html/xcom1.html> (accessed July 3, 2020).
20. <https://nrc-cnrc.github.io/EGSnrc> (accessed July 3, 2020).